49th AIAA/ASME/ASCE/AHS/ASC Structures, Structural Dynamics, and Materials Conference
 16t
7 - 10 April 2008, Schaumburg, IL

AIAA 2008-1797

Check for updates

Least-Squares Continuous Sensitivity Equations for an Infinite Plate with a Hole

Douglas P. Wickert[1], Ronald W. Roberts[1], and Robert A. Canfield[2]
Air Force Institute of Technology, Wright-Patterson AFB, OH, 45433, USA

Continuous sensitivity methods compute design or shape parameter gradients from the continuous system of partial differential equations instead of the discretized system as is more commonly done in multidisciplinary optimization. The continuous sensitivity equations avoid the need to calculate the problematic mesh sensitivities of the discrete method, and are thus more computationally efficient for some applications. Although there exists an extensive body of literature of continuous sensitivity applications for fluid dynamics problems, the application to structural elasticity problems is far more limited, in part due to the complications of determining the stress sensitivity boundary conditions. To partially fill this void, this paper develops and solves the least-squares, continuous sensitivity equations for a classic 2D plane-stress problem. The continuous sensitivity system equations and sensitivity boundary conditions are derived and the problem is posed in first-order form. The problem is solved using a least-squares finite element method incorporating higher-order polynomial elements. The least-squares and continuous results are presented and compared to the analytic solution and analytic sensitivities.

Downloaded by USAF ACADEMY MCDERMOTT LIBR. on November 30, 2021 | http://arc.aiaa.org | DOI: 10.2514/6.2008-1797

I. Introduction

Design sensitivity methods can be grouped into numerical approximate methods or analytic and semi-analytic methods as indicated in Figure 1 . Analytic and semi-analytic methods can be further classified as either discrete or continuous, the difference depending on the order of the discretization and differentiation steps [1, 2]. The most common approach is to discretize the system first and calculate sensitivities by either direct or adjoint methods. For shape sensitivity problems in which the boundary and domain of the problem vary with shape design parameters, the mesh sensitivity must also be calculated for the discrete method which can be problematic. In continuous sensitivity analysis, the design parameter gradients are calculated from the continuous equations yielding a system of differential equations, the continuous sensitivity equations (CSE), governing the sensitivity variables, which are, in turn, discretized and solved [3]. Since the CSE system is posed as a continuous system, it can efficiently produce shape parameter gradients without needing to invert the mesh Jacobian as required by discrete sensitivity method. The CSE system is always a linear system of equations, even when the original system is nonlinear. This can ease the computational burden for some proposed applications, e.g. design sensitivity calculations of transient, nonlinear aeroelasticity problems [4].

Overall, shape sensitivity and optimization methods are more mature for structural problems [5] than they are for fluid problems, but they have not typically employed continuous sensitivity methods [2, 6]. Although there now exists an extensive body of literature describing and documenting the application of continuous sensitivity methods to fluid dynamics problems, the applications to non-fluid problems have largely been limited to 1D scalar problems (e.g. heat flow) and 1D beam problems [6]. Phelan and Haber present a FEM solution for the sensitivity of a 2D structural elasticity problem [7], but much of the remaining literature presents structural CSE theory without any

The views expressed in this paper are those of the author and do not reflect the official policy or position of the United States Air Force, Department of Defense, or the United States Government.

[1] PhD Student, Department of Aeronautical and Astronautical Engineering, 2950 Hobson Way, Wright-Patterson AFB, OH 45433-7765, AIAA Student Member.

[2] Associate Professor, Department of Aeronautical and Astronautical Engineering, 2950 Hobson Way, Wright-Patterson AFB, OH 45433-7765, AIAA Member Grade.

This material is declared a work of the U.S. Government and is not subject to copyright protection in the United States.

representative example problems. The dearth of structural elasticity applications probably stems from the complications involved in determining the appropriate boundary conditions for the sensitivity stress tensor [8, 9]. We are aware of no examples in the literature which employ least-squares finite element methods (LSFEM) to solve the CSE system.

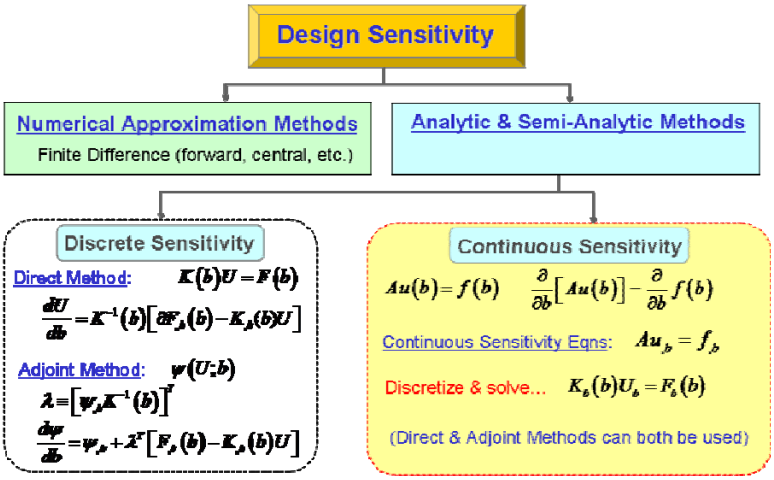

Figure 1 Classification and methods of design sensitivity analysis

The LSFEM method is in the class of weighted residual variational solutions to partial differential equations and has seen a renaissance of interest in the last several years: [10-19] are representative of the range of applications.

This paper begins with a brief description of the LSFEM computational approach used to solve the 2D plane elasticity system and continuous sensitivity equation system. The sensitivity boundary conditions based on a boundary parameterization technique are derived. A classic elasticity problem of an unstressed circular hole in an infinite plate is then introduced and solved using the LSFEM. The CSE boundary conditions are calculated from the gradients of the LSFEM solution and the CSE system is then solved using LSFEM. Advantages of higher-order *p*-elements are discussed. The least-squares, continuous sensitivity results are presented and compared to closed-form analytic gradients.

II. Least-Squares Finite Element Method

Considering the following general boundary value system defined in a domain Ω with a boundary Γ for which we seek a solution $\mathbf{u}$

$$\mathbf{Au} = \mathbf{f} \text{ in } \Omega \tag{1}$$

$$\mathbf{Bu} = \mathbf{g} \text{ on } \Gamma \tag{2}$$

$\mathbf{A}$ is a first-order, time-space differential operator given by

$$\mathbf{A} = \mathbf{A}_t \frac{\partial}{\partial t} + \sum_{i=1}^{\dim} \mathbf{A}_i \frac{\partial}{\partial x_i} + \mathbf{A}_0 \tag{3}$$

$\mathbf{B}$, the boundary operator, has the form

$$\mathbf{B} = \mathbf{B}_t \frac{\partial}{\partial t} + \mathbf{B}_1 \frac{\partial}{\partial \xi_i} + \mathbf{B}_0 \tag{4}$$

where ξ is a coordinate that parameterizes the boundary (e.g. arc length). The square of the system weighted residuals defines a functional

$$J(\mathbf{u};\mathbf{f},\mathbf{g}) = \alpha \left\| \mathbf{Au} - \mathbf{f} \right\|_{\Omega}^2 + (1-\alpha) \left\| \mathbf{Bu} - \mathbf{g} \right\|_{\Gamma}^2 \tag{5}$$

where

Downloaded by USAF ACADEMY MCDERMOTT LIBR. on November 30, 2021 | http://arc.aiaa.org | DOI: 10.2514/6.2008-1797

$$\|\cdot\|_{\Omega}^2 \equiv \int_{\Omega} (\cdot)^2 d\Omega \geq 0 \quad \text{and} \quad \|\cdot\|_{\Gamma}^2 \equiv \int_{\Gamma} (\cdot)^2 d\Gamma \geq 0 \tag{6}$$

are the L^2 norms and $0 < \alpha < 1$ are residual weighting factors. A necessary condition for **u** to minimize (5) is that the first variation of (5) vanishes at **u** [20]. This yields an equivalent bilinear/linear inner product form [21] for the boundary value system (1)-(2)

$$B_{\Omega}(\mathbf{u}, \mathbf{v}) = l_{\Omega}(\mathbf{f}, \mathbf{v}) \quad \forall \mathbf{v} \in \mathbf{V} \tag{7}$$

where

$$\begin{aligned} B_{\Omega}(\mathbf{u}, \mathbf{v}) &\equiv (\mathbf{A}\mathbf{u}, \mathbf{A}\mathbf{v}) \\ l_{\Omega}(\mathbf{f}, \mathbf{v}) &\equiv (\mathbf{f}, \mathbf{A}\mathbf{v}) \end{aligned} \tag{8}$$

and

$$\begin{aligned} B_{\Gamma}(\mathbf{u}, \mathbf{v}) &\equiv (\mathbf{B}\mathbf{u}, \mathbf{B}\mathbf{v}) \\ l_{\Gamma}(\mathbf{g}, \mathbf{v}) &\equiv (\mathbf{g}, \mathbf{B}\mathbf{v}) \end{aligned} \tag{9}$$

For our present effort, $\mathbf{V} \subseteq L_2(\Omega)$, the *Lebesque* space consisting of square integrable functions; or $\mathbf{V} \subseteq H^1(\Omega)$, the basic *Sobolev* space (a *Hilbert* space with first-order derivatives defined) [22]. The appropriate function spaces for the 2D plane elasticity system considered below are $u_i^s \in H^1(\Omega)$ for displacement and $\sigma^s \in H(div;\ \Omega)$ for the stress tensor. Restriction of the stress tensor from the domain to a surface stress vector is the image of the plane stress transformation mapping. As a result, the appropriate boundary function space is $\boldsymbol{\sigma}^s \cdot \mathbf{n}^s \in H^{-1/2}(\Gamma)^2$ for the stress vector [23]. Since it is inconvenient to use the fractional norms, L^2 norms will be substituted in the boundary integral evaluation using a mesh weighting factor

$$\| \cdot \|_{-1/2,\Gamma} \sim h^{1/2} \| \cdot \|_{L^2,\Gamma} \tag{10}$$

where h is a measure of the mesh size.

The domain will be partitioned into finite elements and in each element, we approximate the solution **u** by

$$\mathbf{u} \approx \mathbf{u}_h^e = \sum_{j=1}^{n_{dof}^e} \psi_j \begin{bmatrix} u_1 \ldots u_{n_{nodes}} & a_1 \ldots a_{n_a} & b_1 \ldots b_{n_a} \end{bmatrix}^T \tag{11}$$

where ψ_j are shape functions [24]. The element degrees of freedom, $n_{dof}^e = n_{nodes} + n_a + n_b$, consist of the element nodal values, $u_1 \ldots u_{n_{nodes}}$, the edge coefficients, $a_1 \ldots a_{n_a}$, and the interior (bubble) mode coefficients, $b_1 \ldots b_{n_a}$. This set of degrees of freedom assumes a higher-order hierarchal expansion of shape functions [25]. In what follows, we adopt Szabo's quadrilateral shape function expansion basis which is a serendipity expansion built of kernel functions constructed from Legendre polynomials [26]. Another commonly used expansion consisting of complete polynomials is based on a tensor product expansion of Legendre polynomials in two dimensions [27].

Substituting (11) into (8) yields n_{dof}^e algebraic equations which are evaluated to determine the element stiffness matrix and equivalent force vector

$$\mathbf{K}^e = \int_{\Omega^e} \left(\mathbf{A}\psi_1, ..., \mathbf{A}\psi_{n_{dof}^e} \right)^T \left(\mathbf{A}\psi_1, ..., \mathbf{A}\psi_{n_{dof}^e} \right) d\Omega \tag{12}$$

$$\mathbf{F}^e = \int_{\Omega^e} \left(\mathbf{A}\psi_1, ..., \mathbf{A}\psi_{n_{dof}^e} \right)^T \mathbf{f}\ d\Omega \tag{13}$$

Downloaded by USAF ACADEMY MCDERMOTT LIBR. on November 30, 2021 | http://arc.aiaa.org | DOI: 10.2514/6.2008-1797

$$\mathbf{K}_{\Gamma}^{e} = \int_{\Gamma^e} \left(\mathbf{B}\psi_1, ..., \mathbf{B}\psi_{n_{dof}^e} \right)^T \left(\mathbf{B}\psi_1, ..., \mathbf{B}\psi_{n_{dof}^e} \right) d\Gamma \tag{14}$$

$$\mathbf{G}^{e} = \int_{\Gamma^e} \left(\mathbf{B}\psi_1, ..., \mathbf{B}\psi_{n_{dof}^e} \right)^T \mathbf{g}\, d\Gamma \tag{15}$$

The element stiffness and load vectors are assembled into a global system based on a global degree-of-freedom table. The global system then has the form

$$\left[\alpha\mathbf{K} + (1-\alpha)\mathbf{K}_{\Gamma} \right]\mathbf{u} = \alpha\mathbf{F} + (1-\alpha)\mathbf{G} \tag{16}$$

A. LSFEM Formulations for Elasticity

The published variational formulations of LSFEM for elasticity problems can be classified in three general groups [10]:

1) Perturbed Stokes system: velocity-pressure-vorticity (displacement flux, displacement, curl free constraint)

2) Displacement/displacement gradient (strain)

3) Displacement/stress

All are mixed-elements due to first-order decomposition (a practical necessity for LSFEM implementation). The first method [15] is a div-curl decomposition of the perturbed-form of the Stokes equations and is augmented by pressure and displacement gradient variables. Components of the stress tensor are derived from the displacement fluxes and are not directly available as system variables. Another pressure-displacement method is introduced in [13] which builds upon the use of the -1 norm, $\|\phi\|_{-1} = \sup_{0 \neq \psi \in H^1(\psi)} \frac{(\phi, \psi)}{\|\psi\|_1}$, for the elasticity residual developed in [28]. Although not widely cited, the −1 norm is also used in a stress-displacement and stress-pressure-displacement first-order LSFEM formulations of [12, 29]. The −1 norm allows second-order derivatives to appear in the residual while still using C^0 shape functions, however continuity of stress components across elements is forfeit. As with formulation 3) above, the approach does have the advantage for elasticity boundary value problems in that the implemented variables are displacement and stress which are the primary variables of interest for our coupled FSI approach.

Both formulations 2) and 3) above require special treatment of the symmetry of the strain or stress tensor. One option [30, 31] enforces the symmetry weakly and carries as additional variables each of the off diagonal (theoretically equal) components of the symmetric tensor. This is done at the expense of additional degrees of freedom. Another option is to only carry one each of the off-diagonal components of the stress tensor. This leads to an odd number of variables which destroys the ellipticity of the elasticity system, however, it represents the minimum number of degrees of freedom required to formulate an element approximation. Preliminary results indicate that although the system is no longer elliptic for these formulations, the convergence rate does not suffer when compared to an equivalent number of degrees of freedom [32].

Although LSFEM are theoretically not constrained by the stability problems associated with Galerkin mixed-elements [33], our experience is that LSFEM mixed stress-displacement elements for elasticity can still be beset by problems of slow convergence. Much of this probably stems from the non-coercivity of the implemented forms. (A coercive bilinear form is equivalent to an inner product in the underlying function space. The implication of a coercive formulation is that the existence and uniqueness of variational solutions can be established using the Lax-Milgram variation of the Riesz representation theorem from functional analysis [22].) Poor convergence properties of the LSFEM solution for the non-elliptic mixed stress-displacement formulation appear to be mitigated by using higher-order *p*-elements.

B. First-order 2D Plane Stress Equations

The non-elliptic, mixed stress-displacement formulation requires the minimum number of degrees of freedom (five) to formulate a first-order approximation for the two-dimensional elasticity equations. The mixed stress-

Downloaded by USAF ACADEMY MCDERMOTT LIBR. on November 30, 2021 | http://arc.aiaa.org | DOI: 10.2514/6.2008-1797

displacement unknowns are the three components of the stress tensor, σ_{ij}, and the two components of the displacement vector, u and v. The 2D kinematic relations for elasticity relate the strain tensor components, ε_{ij}, to the gradients of the displacement

$$\begin{aligned} \varepsilon_{xx} &= u_{,x} \\ \varepsilon_{yy} &= v_{,y} \\ \varepsilon_{xy} &= \tfrac{1}{2}\left(u_{,y} + v_{,x}\right) \end{aligned} \tag{17}$$

Assuming a plane-stress state and substituting (17) into the constitutive relation for isotropic Hookean strain

$$\begin{bmatrix} \sigma_{xx} \\ \sigma_{yy} \\ \sigma_{xy} \end{bmatrix} = \frac{E}{1-\nu^2} \begin{bmatrix} 1 & \nu & 0 \\ \nu & 1 & 0 \\ 0 & 0 & \tfrac{1}{2}(1-\nu) \end{bmatrix} \begin{bmatrix} \varepsilon_{xx} \\ \varepsilon_{yy} \\ \varepsilon_{xy} \end{bmatrix} \tag{18}$$

yields three equations relating the stress and the displacements

$$\begin{aligned} \sigma_{xx} &= \frac{E}{1-\nu^2}\left[u_{,x} + \nu v_{,y}\right] \\ \sigma_{yy} &= \frac{E}{1-\nu^2}\left[\nu u_{,x} + v_{,y}\right] \\ \sigma_{xy} &= \frac{E}{4(1+\nu)}\left[u_{,y} + v_{,x}\right] \end{aligned} \tag{19}$$

The two components of the equilibrium equations give the final two equations

$$\begin{aligned} -\rho\, u_{,tt} + \sigma_{xx,x} + \sigma_{xy,y} &= -f_x \\ -\rho\, v_{,tt} + \sigma_{yy,y} + \sigma_{xy,x} &= -f_y \end{aligned} \tag{20}$$

Thus, the 2D plane stress stress-displacement first order system in matrix operator form

$$A_t^s \mathbf{u}_{,tt}^s + A_0^s \mathbf{u}^s + A_1^s \mathbf{u}_{,x}^s + A_2^s \mathbf{u}_{,y}^s = \mathbf{f}^s \tag{21}$$

is

$$\begin{aligned} A_t^s &= \begin{bmatrix} 0 & 0 & 0 & 0 & 0 \\ 0 & 0 & 0 & 0 & 0 \\ 0 & 0 & 0 & 0 & 0 \\ -\rho^s & 0 & 0 & 0 & 0 \\ 0 & -\rho^s & 0 & 0 & 0 \end{bmatrix} \quad A_0^s = \begin{bmatrix} 0 & 0 & 1 & 0 & 0 \\ 0 & 0 & 0 & 1 & 0 \\ 0 & 0 & 0 & 0 & 1 \\ 0 & 0 & 0 & 0 & 0 \\ 0 & 0 & 0 & 0 & 0 \end{bmatrix} \\ A_1^s &= \begin{bmatrix} \frac{-E}{1-\nu^2} & 0 & 0 & 0 & 0 \\ \frac{-\nu E}{1-\nu^2} & 0 & 0 & 0 & 0 \\ 0 & \frac{-E}{4(1+\nu)} & 0 & 0 & 0 \\ 0 & 0 & 1 & 0 & 0 \\ 0 & 0 & 0 & 0 & 1 \end{bmatrix} \quad A_2^s = \begin{bmatrix} 0 & \frac{-\nu E}{1-\nu^2} & 0 & 0 & 0 \\ 0 & \frac{-E}{1-\nu^2} & 0 & 0 & 0 \\ \frac{-E}{4(1+\nu)} & 0 & 0 & 0 & 0 \\ 0 & 0 & 0 & 0 & 1 \\ 0 & 0 & 0 & 1 & 0 \end{bmatrix} \quad \mathbf{f}^s = \begin{bmatrix} 0 \\ 0 \\ 0 \\ -f_x \\ -f_y \end{bmatrix} \end{aligned} \tag{22}$$

where $\mathbf{u}^s = \begin{bmatrix} u & v & \sigma_{xx} & \sigma_{yy} & \sigma_{xy} \end{bmatrix}^T$. The s superscripts are introduced to denote structure domain variables.

Downloaded by USAF ACADEMY MCDERMOTT LIBR. on November 30, 2021 | http://arc.aiaa.org | DOI: 10.2514/6.2008-1797

As discussed above, formulation (22) has an odd number of variables and thus can no longer be elliptic even though elasticity systems are elliptic in nature. Additionally, this formulation is not coercive in H^1. The choice of this formulation for LSFEM is based primarily on the minimum number of degrees of freedom required and the presence of the stress tensor allowing direct access to traction boundary conditions and stress sensitivity.

III. Continuous Sensitivity Equations

The continuous sensitivity method differentiates the continuous system to yield a governing system of equations for the sensitivity variables. For example, differentiating some governing field equations with respect to a design parameter, b

$$\frac{\partial}{\partial b}\left[A_t \mathbf{u}_{,tt} + A_0 \mathbf{u} + A_1 \mathbf{u}_{,x} + A_2 \mathbf{u}_{,y} \right] = \frac{\partial}{\partial b}\left[\mathbf{f} \right] \tag{23}$$

$$A_t \frac{\partial}{\partial b}\frac{\partial^2 \mathbf{u}}{\partial t^2} + A_0 \frac{\partial}{\partial b}\mathbf{u} + A_1 \frac{\partial}{\partial b}\frac{\partial \mathbf{u}}{\partial x} + A_2 \frac{\partial}{\partial b}\frac{\partial \mathbf{u}}{\partial y} = \frac{\partial \mathbf{f}}{\partial b} \tag{24}$$

$$A_t \left({}^b\mathbf{u}_{,tt} \right) + A_0 \left({}^b\mathbf{u} \right) + A_1 \left({}^b\mathbf{u}_{,x} \right) + A_2 \left({}^b\mathbf{u}_{,y} \right) = 0 \tag{25}$$

Since the spatial-temporal derivatives are independent operations from the sensitivity derivative, the order of differentiation may be reversed. Now, for example, defining the E-B Beam structure sensitivity variables as

$${}^b\mathbf{u}^s \equiv \frac{\partial}{\partial b}\mathbf{u}^s = \begin{bmatrix} u^s_{,b} & v^s_{,b} & \sigma^s_{xx,b} & \sigma^s_{yy,b} & \sigma^s_{xy,b} \end{bmatrix}^T \tag{26}$$

yields the final CSE system

$$A^s_t \left({}^b\mathbf{u}^s_{,t} \right) + A^s_0 \left({}^b\mathbf{u}^s \right) + A^s_1 \left({}^b\mathbf{u}^s_{,x} \right) + A^s_2 \left({}^b\mathbf{u}^s_{,y} \right) = 0 \tag{27}$$

The CSE may now be discretized and solved using the same LSFEM method used to solve the elasticity system. The continuous sensitivity system is thus simply another system of differential equations which, together with the appropriate boundary data, represents a well-conditioned boundary value problem which may be solved by any of a wide variety of numerical approaches. It is convenient in many cases to use the same numerical method/framework to solve the sensitivity system as was used to solve the original system.

The sensitivity equation boundary conditions specify how the sensitivity variables behave on the boundary of the domain. For shape variation problems, there are two ways in which boundary values for a scalar or vector field variable (considered component-wise), u, may change on the boundary. First, the boundary condition of the original problem may be altered by a change in the design parameter. Second, the design parameter may alter the shape of the boundary and domain and thus the value of the field variable. These are related through the concept of the material derivative

$$\left.\frac{Du}{Db}\right|_{\mathbf{X}} = \left.\frac{\partial u}{\partial b}\right|_{\mathbf{x}} + \nabla u \cdot \left.\frac{\partial \mathbf{x}}{\partial b}\right|_{\mathbf{X}} \tag{28}$$

where $\mathbf{X}$ denotes a material coordinate and $\mathbf{x}$ denotes a spatial coordinate (Eulerian description). Thus the total derivative of u with respect to b at a material point $\mathbf{X}_0$ consists of the local derivative of u with respect to parameter b and a transport term which accounts for how the material point $\mathbf{X}_0$ changes character in spatial coordinates as the design parameter b varies. If u is a vector quantity, then the gradient operation and dot product in the advection term are carried out row-wise. The desired sensitivity variable boundary condition for a scalar or vector quantity is thus

$${}^b\mathbf{u}\Big|_\Gamma \equiv \left.\frac{\partial \mathbf{u}}{\partial b}\right|_{\mathbf{X}=\Gamma} = \left.\frac{D\mathbf{u}}{Db}\right|_\Gamma - \nabla \mathbf{u} \cdot \frac{\partial \mathbf{x}_{\Gamma(b)}}{\partial b} \tag{29}$$

The first term on the right side accounts for how the boundary conditions for the problem change with respect to the design parameter. In most cases, this term is zero. That is, the boundary condition does not change as the shape changes. The advection term uses the gradient of the solution. In a finite element solution, this expression comes from the gradient of the shape functions applied to the finite element solution.

Downloaded by USAF ACADEMY MCDERMOTT LIBR. on November 30, 2021 | http://arc.aiaa.org | DOI: 10.2514/6.2008-1797

If the dependent variable is a tensor, as in the case of the fluid or structure stress tensor, then the more complicated upper convected derivative or Oldroyd derivative must be used in place of (28) [34]

$$\mathbf{S}^{\nabla} = \frac{D}{Db}\mathbf{S} - \left(\nabla\frac{\partial \mathbf{x}}{\partial b}\right)^{T}\cdot\mathbf{S} - \mathbf{S}\cdot\left(\nabla\frac{\partial \mathbf{x}}{\partial b}\right) \tag{30}$$

where $\nabla\partial\mathbf{x}/\partial b$ is the tensor of design parameter velocities and $\mathbf{S}$ is a tensor. Equation (30) is equivalent (the comparison is formally considered in a future work [35]) to the stress tensor sensitivity expressed in terms normal and tangential surface tractions derived in a different manner by Dems and Haftka [8]

$${}^{b}\sigma_{ij}^{s}n_j = \frac{DT_i}{Db} - \sigma_{ij,k}n_j\frac{\partial\phi_k}{\partial b} - \sigma_{ij}\left(n_j n_l - \delta_{jl}\right)n_k\left[\frac{\partial\phi_k}{\partial b}\right]_{,l} \tag{31}$$

where tensor index notation has been used, T_i are the components of the surface traction vector, n_i are the components of the unit normal/tangential vector, δ is the delta function, and ϕ is the transformation field that maps material coordinates of the domain as a function of the design parameter

$$\mathbf{x}^{t} = \mathbf{x} + \phi\left(\mathbf{X}; b\right) \tag{32}$$

A variation of the domain due to a variation in design parameter, b, can then be described by

$$\delta\phi_k = \frac{\partial\phi_k}{\partial b}\delta b = {}^{b}v_k\delta b \tag{33}$$

and ${}^{b}\mathbf{v}$ is designated the velocity of the transformation field.

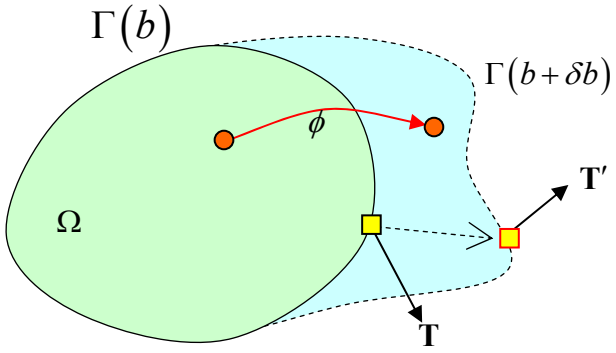

Figure 2 Domain and boundary shape variation

To avoid having to use the more complicated (30) for the stress tensor, we express the stress tensor at points on the boundary surface in terms of the stress vector at that point. For example, in two dimensions [36]

$$\mathbf{T}^{(\hat{\mathbf{n}})} = \begin{Bmatrix} T_n \\ T_s \end{Bmatrix} = \left[\underline{\underline{\sigma}}\right]^{T}\cdot\left\{\hat{\mathbf{n}}\right\} \equiv \begin{Bmatrix} \sigma_n \\ \sigma_t \end{Bmatrix} \tag{34}$$

where the normal and tangential components of the stress vector may also be determined by the coordinate transformation

$$\sigma_n = \sigma_{xx}\cos^2\left(\theta\right) + \sigma_{yy}\sin^2\left(\theta\right) + 2\sigma_{xy}\sin\left(\theta\right)\cos\left(\theta\right) \tag{35}$$

$$\sigma_t = -\left(\sigma_{xx} - \sigma_{yy}\right)\sin\theta\cos\theta + \sigma_{xy}\left(\cos^2\theta - \sin^2\theta\right) \tag{36}$$

This approach is particularly convenient since the surface stress vector can be directly equated to any surface tractions as implied in (34).

To summarize, the continuous sensitivity system is a linear boundary value problem. The constrained variables on a given boundary are the same as for the original problem, however the values for the boundary conditions depend on the gradient of the solution of the original problem. If the variables are scalars or vectors, (29) may be used to determine the boundary values. Tensor expressions are more simply implemented if the tensor expression is

Downloaded by USAF ACADEMY MCDERMOTT LIBR. on November 30, 2021 | http://arc.aiaa.org | DOI: 10.2514/6.2008-1797

transformed to a boundary vector expression for which (29) may then be applied. In some cases, the shape variation may change the function imposed on the boundary (the first term on the right in (29)), but this is rare. The example problem considered next does use this term, but the condition arises from the imposition of "infinite"-domain boundary conditions on a finite domain.

IV. Plane Elasticity CSE Example Problem

The infinite plate with an elliptical hole in Figure 3 is a classic stress concentration problem in elasticity. The plate is loaded in uniaxial tension and the hole is unstressed (i.e. no external load is applied at the hole). Through symmetry we model a quarter of the domain. We consider a finite portion of the quarter domain and impose the analytic normal and tangential stress distribution on boundaries Γ_2 and Γ_3. We first consider the solution of the elasticity system and then the solution to the CSE system.

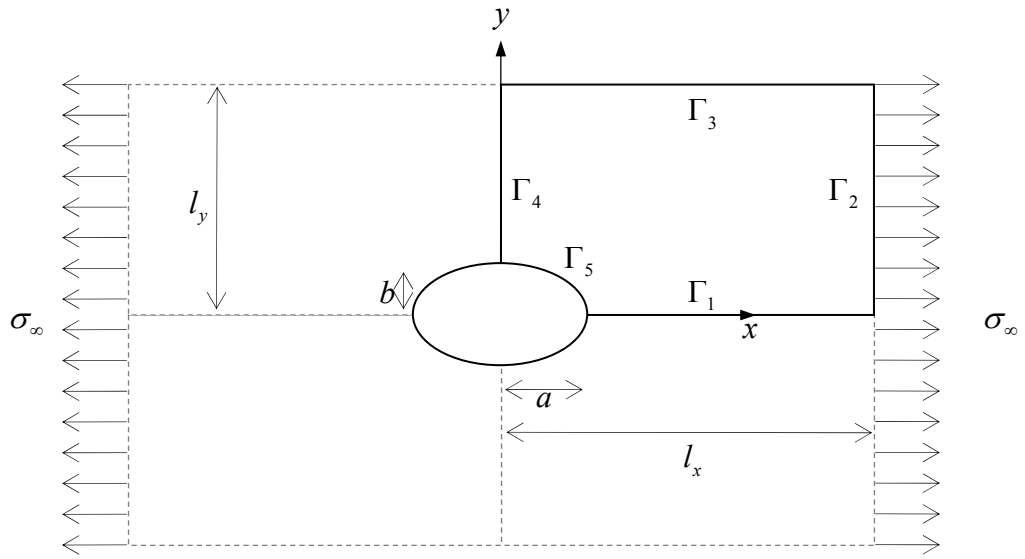

Figure 3 Plate with an elliptical hole

A. Analytic and LSFEM Solution

The analytic stress and displacement solutions for a circular hole are [26]

$$u(r,\theta)=\frac{\sigma_\infty a}{8G}\left[\frac{r}{a}(\kappa+1)\cos\theta+2\frac{a}{r}\left((1+\kappa)\cos\theta+\cos 3\theta\right)-2\frac{a^3}{r^3}\cos 3\theta\right] \tag{37}$$

$$v(r,\theta)=\frac{\sigma_\infty a}{8G}\left[\frac{r}{a}(\kappa-3)\sin\theta+2\frac{a}{r}\left((1-\kappa)\sin\theta+\sin 3\theta\right)-2\frac{a^3}{r^3}\sin 3\theta\right] \tag{38}$$

$$\sigma_{xx}(r,\theta)=\sigma_\infty\left[1-\frac{a^2}{r^2}\left(\frac{3}{2}\cos 2\theta+\cos 4\theta\right)+\frac{3}{2}\frac{a^4}{r^4}\cos 4\theta\right] \tag{39}$$

$$\sigma_{yy}(r,\theta)=\sigma_\infty\left[-\frac{a^2}{r^2}\left(\frac{1}{2}\cos 2\theta-\cos 4\theta\right)-\frac{3}{2}\frac{a^4}{r^4}\cos 4\theta\right] \tag{40}$$

$$\sigma_{xy}(r,\theta)=\sigma_\infty\left[-\frac{a^2}{r^2}\left(\frac{1}{2}\sin 2\theta+\sin 4\theta\right)+\frac{3}{2}\frac{a^4}{r^4}\sin 4\theta\right] \tag{41}$$

Downloaded by USAF ACADEMY MCDERMOTT LIBR. on November 30, 2021 | http://arc.aiaa.org | DOI: 10.2514/6.2008-1797

where $\kappa = (3-\nu)/(1+\nu)$ and the modulus of rigidity, $G = E/(2(1+\nu))$. We take Poisson's ratio, ν = 1/3, and non-dimensionalize the system so that $E = 1$. Boundary conditions are given in 0For a circular hole, a·= b = ¼ and taking $l_x = l_y = 4a = 1$. For $\sigma_\infty = 10$ we obtain the analytic solution in Figure 4 and compare it to the LSFEM solution in Figure 5 .

Plate with a circular hole boundary conditions

Boundary	Boundary Condition
Γ_1	$v = 0, \quad \sigma_{xy} = 0$ plate symmetry
Γ_2	σ_{xx} & σ_{xy} analytic solution
Γ_3	σ_{yy} & σ_{xy} analytic solution
Γ_4	$u = 0, \quad \sigma_{xy} = 0$ plate symmetry
Γ_5	$\sigma_n = 0, \quad \sigma_t = 0$ stress free hole

Downloaded by USAF ACADEMY MCDERMOTT LIBR. on November 30, 2021 | http://arc.aiaa.org | DOI: 10.2514/6.2008-1797

Downloaded by USAF ACADEMY MCDERMOTT LIBR. on November 30, 2021 | http://arc.aiaa.org | DOI: 10.2514/6.2008-1797

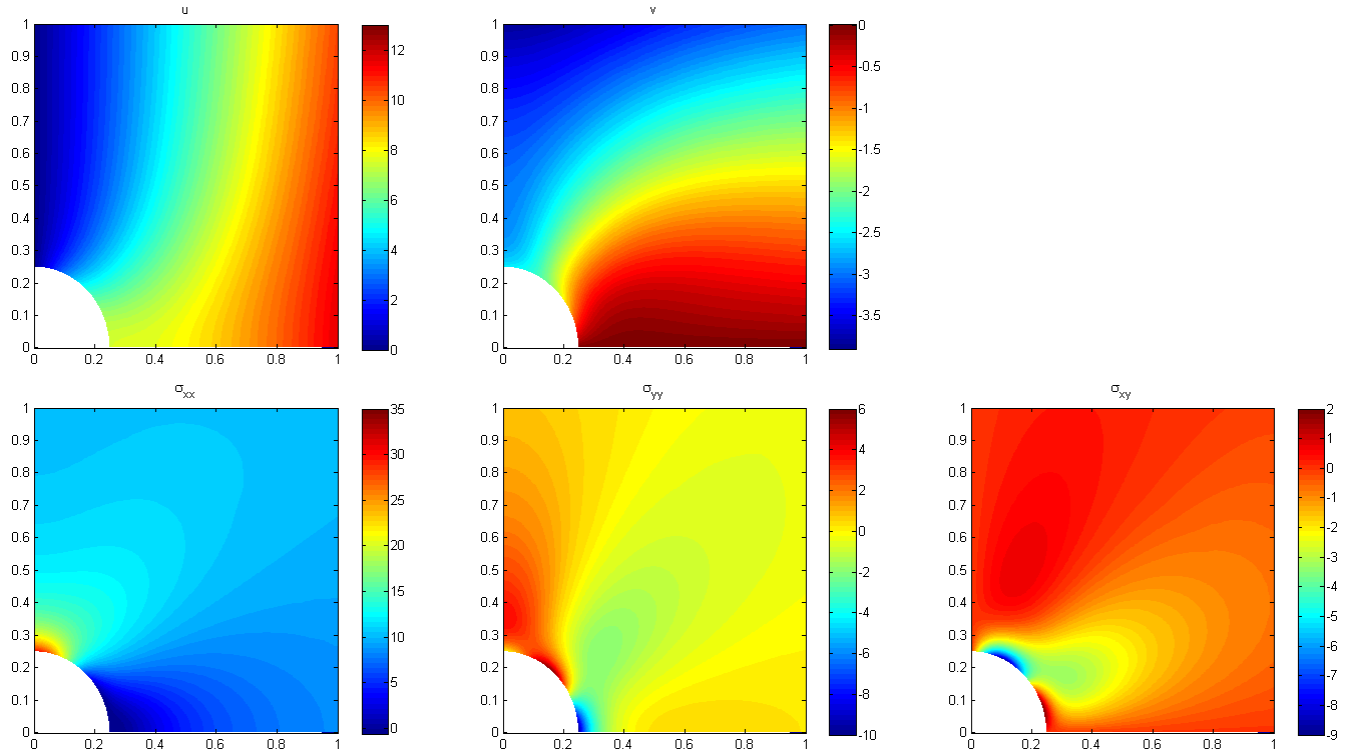

Figure 4 Analytic Solution for Quarter Plate with a circular hole

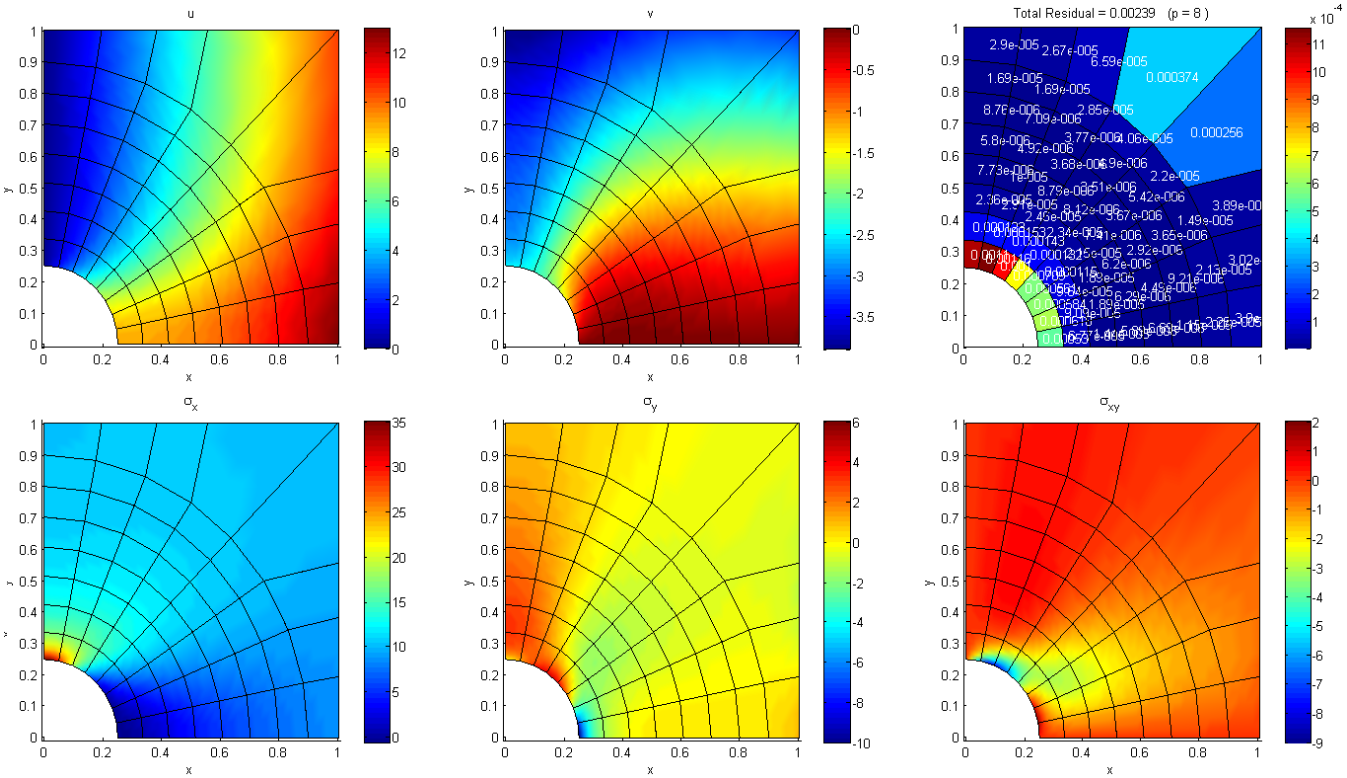

Figure 5 LSFEM Solution for Quarter Plate with a circular hole (p = 8)

In obtaining the solution, the Γ_2, Γ_3, and Γ_5 boundary conditions are weakly enforced using a boundary integral method discussed above. The Γ_2, and Γ_3 boundaries are straightforward as they are in the same coordinate system. For Γ_5, a plane stress transformation is used to construct the stress vector on the hole boundary which is then equated to the stress-free boundary condition. Accurate interpolation on the boundary is possible by using the blending function method [26]. The boundary in the present case is a circle, so a parabolic blending function suffices to completely describe the boundary coordinates as a function of natural coordinates. For the mesh used in the analysis of the present problem, the hole boundary always lies on the fourth side of the standard quadrilateral element. Thus, coordinate interpolation along the hole is

$$\begin{Bmatrix} x \\ y \end{Bmatrix} = \frac{1}{4}(1-\xi)(1+\eta)\begin{Bmatrix} X_2 \\ Y_2 \end{Bmatrix} + \frac{1}{4}(1+\xi)(1+\eta)\begin{Bmatrix} X_3 \\ Y_3 \end{Bmatrix} + \frac{1}{2}(1-\xi)\mathbf{x}_4(\eta) \tag{42}$$

where

$$\mathbf{x}_4(\eta) = \begin{Bmatrix} x_\eta \\ y_\eta \end{Bmatrix} = r_{hole}\begin{Bmatrix} \cos\left[\frac{1}{2}(1-\eta)\theta_1 + \frac{1}{2}(1+\eta)\theta_4\right] \\ \sin\left[\frac{1}{2}(1-\eta)\theta_1 + \frac{1}{2}(1+\eta)\theta_4\right] \end{Bmatrix} \tag{43}$$

and where θ_1 and θ_4 are the polar angles of the first and fourth vertex coordinates and r_{hole} is the hole radius.

B. Analytic Sensitivities and CSE Solution

Since the elasticity equations are linear, the CSE first-order matrix operators are identical to the elasticity system operators. The CSE boundary conditions are calculated from the original boundary condition set and the gradients of the LSFEM solution. Taking hole radius, a, as the shape parameter, the Γ_1, Γ_4, and Γ_5 boundaries change with the hole. The hole coordinates are easily parameterized in polar coordinates as

$$X_{\Gamma_5} = \left\{ \begin{pmatrix} a & \theta \end{pmatrix}^T \right\}_{(r\theta)} \tag{44}$$

so that

$$X_{\Gamma_5,a} = \left\{ \begin{pmatrix} 1 & 0 \end{pmatrix}^T \right\}_{(r\theta)} \tag{45}$$

Similarly, in Cartesian coordinates,

$$X_{\Gamma_1} = \left\{ \left(\begin{bmatrix} 1-\xi & \xi \end{bmatrix} \begin{Bmatrix} a \\ 1 \end{Bmatrix} \quad 0 \right)^T \middle| \, \xi \in [0,1] \right\}_{(xy)} \tag{46}$$

$$X_{\Gamma_4} = \left\{ \left(0 \quad \begin{bmatrix} 1-\xi & \xi \end{bmatrix} \begin{Bmatrix} b \\ 1 \end{Bmatrix} \right)^T \middle| \, \xi \in [0,1] \right\}_{(xy)} \tag{47}$$

Then, for a circular hole with $a = b$

$$X_{\Gamma_1,a} = \left\{ \begin{pmatrix} 1-\xi & 0 \end{pmatrix}^T \middle| \, \xi \in [0,1] \right\}_{(xy)} \tag{48}$$

$$X_{\Gamma_4,a} = \left\{ \begin{pmatrix} 0 & 1-\xi \end{pmatrix}^T \middle| \, \xi \in [0,1] \right\}_{(xy)} \tag{49}$$

Now, differentiating the boundary conditions along Γ_1 and Γ_4 and evaluating the advection term with (48) and (49), (29) yields

$$\begin{Bmatrix} {}^a v(\xi) \\ {}^a \sigma_{xy}(\xi) \end{Bmatrix}_{\Gamma_1} = \frac{D\begin{Bmatrix} v & \sigma_{xy} \end{Bmatrix}_{\Gamma_1}^T}{Da} - \begin{Bmatrix} \nabla v \\ \nabla \sigma_{xy} \end{Bmatrix} \cdot \frac{\partial X_{\Gamma_1}}{\partial a} = 0 - \begin{Bmatrix} (1-\xi) v_{,x} \\ (1-\xi)\sigma_{xy,x} \end{Bmatrix}_{\xi \in [0,1]} = 0 \tag{50}$$

Downloaded by USAF ACADEMY MCDERMOTT LIBR. on November 30, 2021 | http://arc.aiaa.org | DOI: 10.2514/6.2008-1797

$$\left\{\begin{matrix} {}^{a}u(\xi) \\ {}^{a}\sigma_{xy}(\xi) \end{matrix}\right\}_{\Gamma_4} = \frac{D\left\{u \quad \sigma_{xy}\right\}_{\Gamma_4}^{T}}{Da} - \left\{\begin{matrix} \nabla u \\ \nabla \sigma_{xy} \end{matrix}\right\} \cdot \frac{\partial X_{\Gamma_4}}{\partial a} = 0 - \left\{\begin{matrix} (1-\xi)u_{,x} \\ (1-\xi)\sigma_{xy,x} \end{matrix}\right\}_{\xi\in[0,1]} = 0 \tag{51}$$

For Γ_5, the gradients in the advection term must be calculated from the gradients of the LSFEM solution and are not available by inspection as they are for Γ_1 and Γ_4. The Γ_5 CSE boundary conditions are

$$\left\{\begin{matrix} {}^{a}\sigma_{rr} \\ {}^{a}\sigma_{r\theta} \end{matrix}\right\}_{\Gamma_5} = \frac{D\left\{\sigma_{rr} \quad \sigma_{r\theta}\right\}_{\Gamma_5}^{T}}{Da} - \nabla_{(r\theta)} \left\{\begin{matrix} \sigma_{rr} \\ \sigma_{r\theta} \end{matrix}\right\} \cdot \frac{\partial}{\partial a}\left\{X_{\Gamma_5}\right\}_{(r\theta)} = \left\{\begin{matrix} -\sigma_{rr,r} \\ -\sigma_{r\theta,r} \end{matrix}\right\} \tag{52}$$

where is should be noted that the gradient operator and boundary set definition must be expressed in the same coordinate system. The polar coordinate gradient operator

$$\nabla_{(r\theta)} \equiv \left\langle \frac{\partial}{\partial r} \quad \frac{1}{r}\frac{\partial}{\partial \theta} \right\rangle \tag{53}$$

The plane stress transformation relationship may be used to relate the Cartesian and polar stress components along the hole

$$\sigma_n = \sigma_{xx}\cos^2(\theta) + \sigma_{yy}\sin^2(\theta) + 2\sigma_{xy}\sin(\theta)\cos(\theta) \tag{54}$$

$$\sigma_t = -(\sigma_{xx} - \sigma_{yy})\sin\theta\cos\theta + \sigma_{xy}(\cos^2\theta - \sin^2\theta) \tag{55}$$

The radial gradients of the normal and tangential stress components are

$$\sigma_{rr,r} = \sigma_{xx,r}\cos^2(\theta) + \sigma_{yy,r}\sin^2(\theta) + 2\sigma_{xy,r}\sin(\theta)\cos(\theta) \tag{56}$$

$$\sigma_{r\theta,r} = -(\sigma_{xx,r} - \sigma_{yy,r})\sin\theta\cos\theta + \sigma_{xy,r}(\cos^2\theta - \sin^2\theta) \tag{57}$$

Using the chain rule

$$\frac{d}{dr}(\cdot) = \frac{\partial(\cdot)}{\partial x}\frac{\partial x}{\partial r} + \frac{\partial(\cdot)}{\partial y}\frac{\partial y}{\partial r} \tag{58}$$

and noting by the definition of polar coordinates that

$$x_{,r} = \cos\theta \tag{59}$$

$$y_{,r} = \sin\theta \tag{60}$$

yields the radial stress CSE boundary condition in terms of Cartesian gradients

$$\begin{aligned} {}^{a}\sigma_{rr} = -\sigma_{rr,r} = &-(\sigma_{xx,x}\cos\theta + \sigma_{xx,y}\sin\theta)\cos^2\theta + \ldots \\ &-(\sigma_{yy,x}\cos\theta + \sigma_{yy,y}\sin\theta)\sin^2\theta + \ldots \\ &-2(\sigma_{xy,x}\cos\theta + \sigma_{xy,y}\sin\theta)\cos\theta\sin\theta \end{aligned} \tag{61}$$

Similarly, the tangential CSE traction condition is

$$\begin{aligned} {}^{a}\sigma_{r\theta} = -\sigma_{r\theta,r} = &\left[(\sigma_{xx,x} - \sigma_{yy,x})\cos\theta + (\sigma_{xx,y} - \sigma_{yy,y})\sin\theta\right]\cos\theta\sin\theta + \ldots \\ &-(\sigma_{xy,x}\cos\theta + \sigma_{xy,y}\sin\theta)(\cos^2\theta - \sin^2\theta) \end{aligned} \tag{62}$$

The gradients of the Cartesian stress components required in (61) and (62) come from the LSFEM solution by evaluating gradients of the shape functions.

Analytic sensitivity expressions are calculated by differentiating (39) thru (41) with respect to the hole radius

Downloaded by USAF ACADEMY MCDERMOTT LIBR. on November 30, 2021 | http://arc.aiaa.org | DOI: 10.2514/6.2008-1797

$$\sigma_{xx,r}\Big|_{r=a} = \sigma_\infty \left[\frac{1}{a}\left(3\cos 2\theta + 2\cos 4\theta\right) - \frac{6}{a}\cos 4\theta \right] \tag{63}$$

$$\sigma_{yy,r}\Big|_{r=a} = \sigma_\infty \left[\frac{1}{a}\left(\cos 2\theta - 2\cos 4\theta\right) + \frac{6}{a}\cos 4\theta \right] \tag{64}$$

$$\sigma_{xy,r}\Big|_{r=a} = \sigma_\infty \left[\frac{1}{a}\left(\sin 2\theta + 2\sin 4\theta\right) - \frac{6}{a}\sin 4\theta \right] \tag{65}$$

This analytic expression is compared to the LSFEM-derived (p = 8 LSFEM solution) CSE stress boundary conditions in Figure 6 . Overall, the agreement is better for the radial sensitivity than for the tangential sensitivity. This primarily stems from the greater error present in the tangential stress component that is apparent in the LSFEM solution along Γ_5 plotted in Figure 8 . The shape functions employed in the LSFEM are C^0 shape functions and the discontinuity between elements is apparent in Figure 8 . It has been conjectured that writing the LS functional and evaluating the element stiffness matrices in terms of the H^1 norm in lieu of the L^2 norm may improve the approximation of the gradient of the solution. This would in turn improve the accuracy of the CSE boundary conditions. This flexibility in norm choice is an advantage of the LSFEM as implemented.

An analytic sensitivity expression for the entire domain is obtained by differentiating (37) - (41) with respect to hole radius, a. The analytic sensitivities are

$${}^a u \equiv u_{,a} = \frac{\sigma_\infty}{8G}\left[4\frac{a}{r}\left(\left(1+\kappa\right)\cos\theta + \cos 3\theta\right) - 8\frac{a^3}{r^3}\cos 3\theta \right] \tag{66}$$

$${}^a v \equiv v_{,a} = \frac{\sigma_\infty}{8G}\left[4\frac{a}{r}\left(\left(1-\kappa\right)\sin\theta + \sin 3\theta\right) - 8\frac{a^3}{r^3}\sin 3\theta \right] \tag{67}$$

$${}^a \sigma_{xx} \equiv \sigma_{xx,a} = \sigma_\infty \left[-\frac{a}{r^2}\left(3\cos 2\theta + 2\cos 4\theta\right) + 6\frac{a^3}{r^4}\cos 4\theta \right] \tag{68}$$

$${}^a \sigma_{yy} \equiv \sigma_{yy,a} = \sigma_\infty \left[-\frac{a}{r^2}\left(\cos 2\theta - 2\cos 4\theta\right) - 6\frac{a^3}{r^4}\cos 4\theta \right] \tag{69}$$

$${}^a \sigma_{xy} \equiv \sigma_{xy,a} = \sigma_\infty \left[-\frac{a}{r^2}\left(\sin 2\theta + 2\sin 4\theta\right) + 6\frac{a^3}{r^4}\sin 4\theta \right] \tag{70}$$

The analytic hole radius sensitivities are plotted in Figure 8 and compared to the LS CSE solution in Figure 9 . Overall, the agreement is very good and the boundary parameterization approach for determining the CSE boundary conditions from the LSFEM solution appears very promising. For the circular hole considered here, the boundary parameterization was very simple. However, there are no theoretical reasons to expect the method would not work equally as well for more complicated boundaries. Even boundaries that cannot be represented as polynomial curves can be approximated by a polynomial by any of the various higher-order spline techniques. This will be explored in future work.

Downloaded by USAF ACADEMY MCDERMOTT LIBR. on November 30, 2021 | http://arc.aiaa.org | DOI: 10.2514/6.2008-1797

Downloaded by USAF ACADEMY MCDERMOTT LIBR. on November 30, 2021 | http://arc.aiaa.org | DOI: 10.2514/6.2008-1797

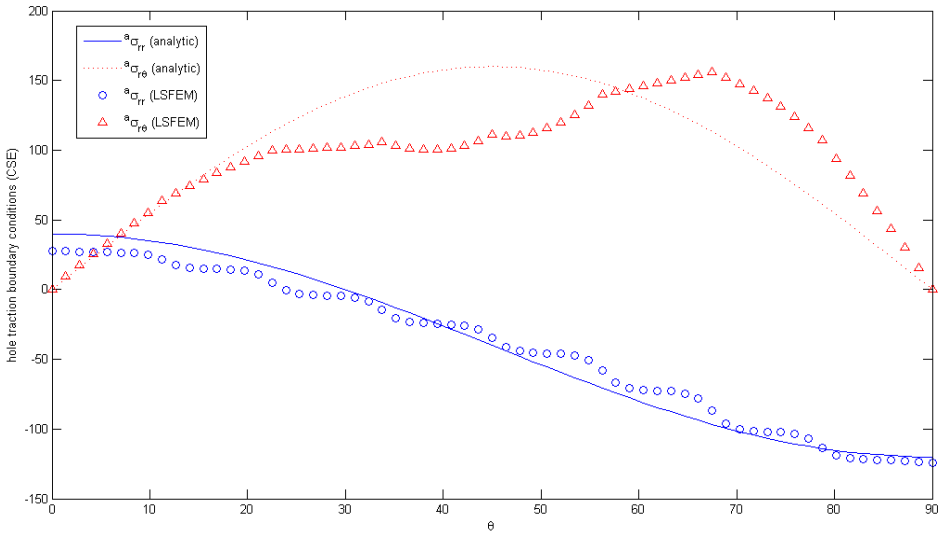

Figure 6 Comparison of analytic and LSFEM-derived sensitivity boundary conditions

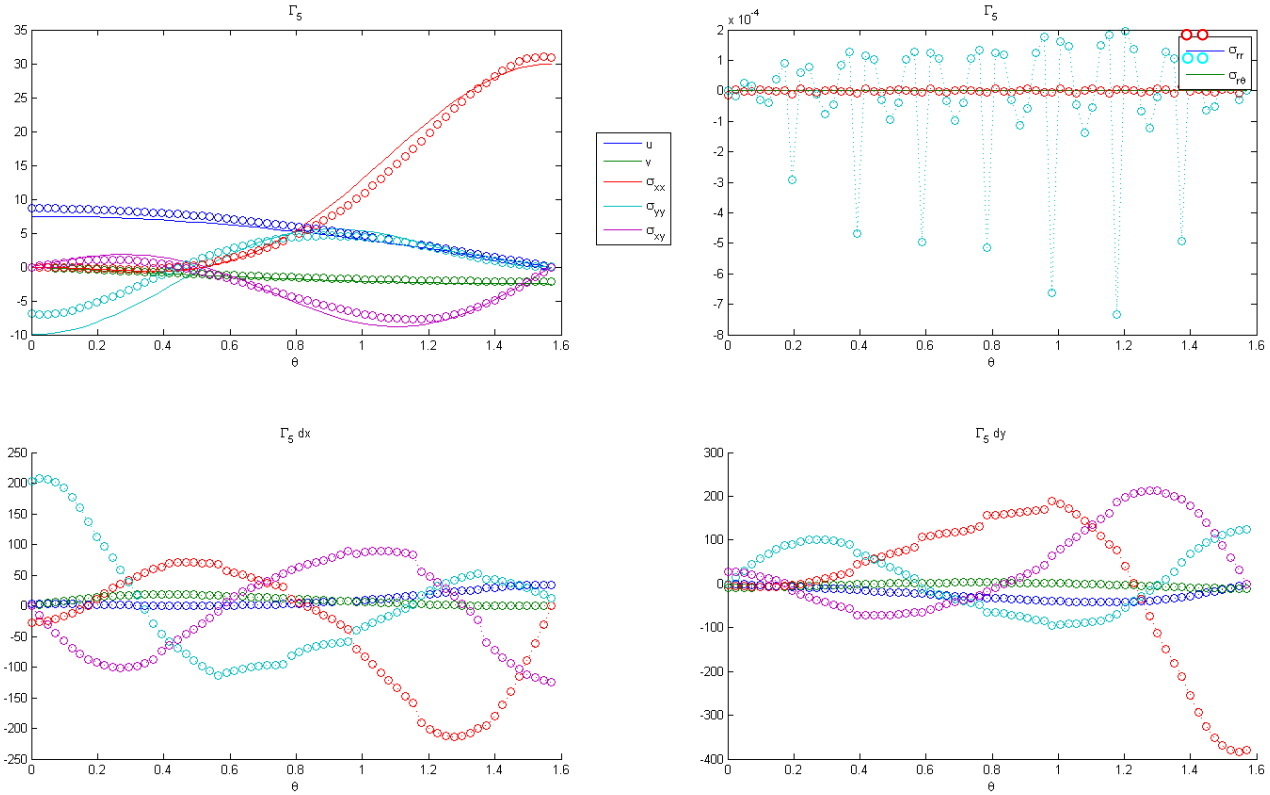

Figure 7 Comparison of analytic and LSFEM solutions along the hole boundary

Downloaded by USAF ACADEMY MCDERMOTT LIBR. on November 30, 2021 | http://arc.aiaa.org | DOI: 10.2514/6.2008-1797

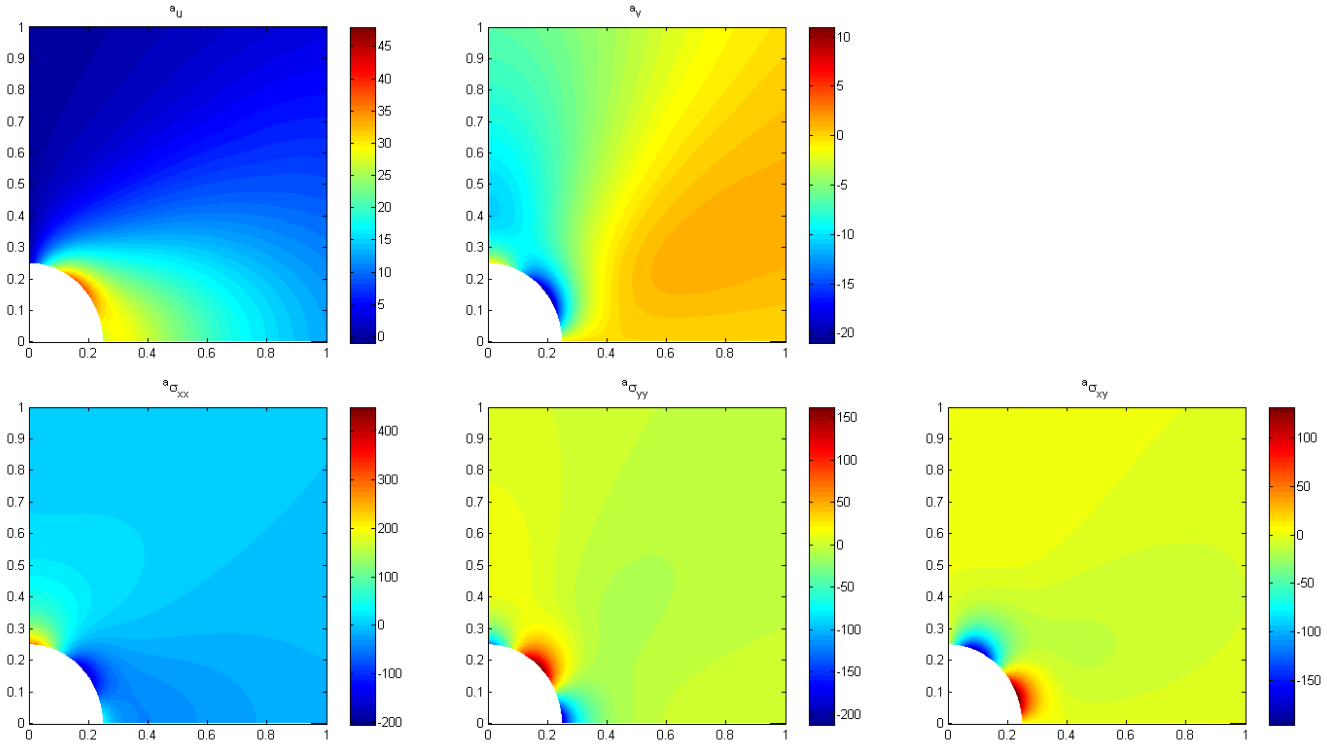

Figure 8 Analytic Sensitivity Solution for Quarter Plate with a circular hole

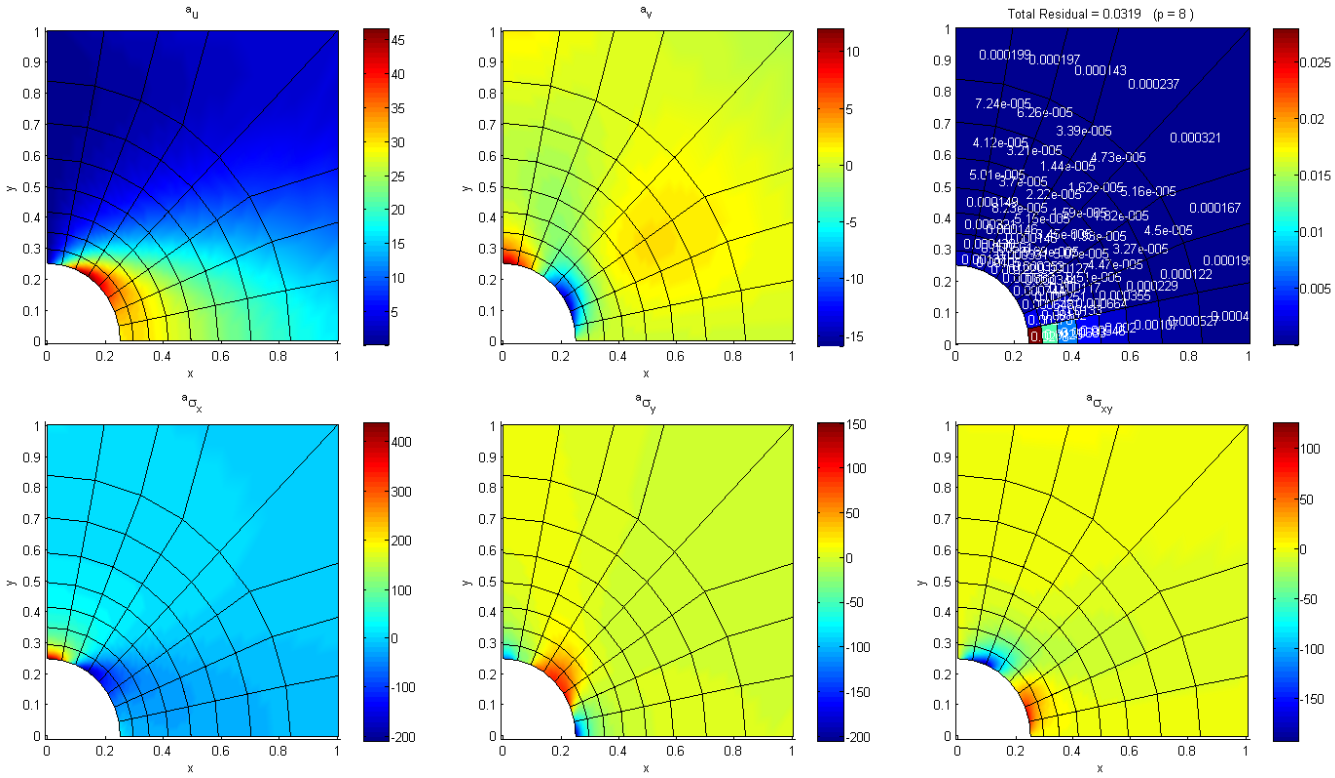

Figure 9 LSFEM Solution for Quarter Plate with a circular hole (p = 8)

V. Conclusion

A least-squares continuous sensitivity analysis method was developed for two-dimensional plane elasticity. The problem was posed in a first-order plane stress-displacement LSFEM formulation. Because the elasticity system is linear, the differential operator form for the elasticity and continuous sensitivity system are identical. The CSE sensitivity boundary conditions were derived by transforming the stress tensor into a surface stress vector on a properly parameterized boundary. Gradients of the LSFEM solution then permitted a straightforward method for specifying the CSE boundary conditions. This obviated the need to use a far more complicated expansion of the stress tensor sensitivity expression available in the literature. It is presumed that the complications associated with the stress tensor sensitivity expression are what have prevented the application of continuous sensitivity analysis methods to structural systems. A fairly simple example problem was posed and solved and the least-squares CSE results very closely matched the analytic sensitivities. The boundary parameterization and stress vector approach developed here should be generalizable to more complicated boundaries.

Downloaded by USAF ACADEMY MCDERMOTT LIBR. on November 30, 2021 | http://arc.aiaa.org | DOI: 10.2514/6.2008-1797

VI. Acknowledgements

The Air Force Office of Scientific Research funded this research, contract number F1ATA07337J001. The authors gratefully acknowledge the support of the computational mathematics program manager, Dr. Fariba Fahroo.

VII. References

[1] Haug, E.J., Choi, K.K., and Komkov, V., "Design sensitivity analysis of structural systems," *Mathematics in science and engineering,* Vol. 177, Academic Press, Orlando, 1986, pp. 381.

[2] Choi, K.K., and Kim, N.H., "Structural sensitivity analysis and optimization," *Mechanical engineering series,* Springer Science+Business Media, New York, 2005.

[3] Borggaard, J., and Burns, J., "A PDE Sensitivity Equation Method for Optimal Aerodynamic Design," *Journal of Computational Physics,* Vol. 136, 1997, pp. 366--384.

[4] Wickert, D.P., and Canfield, R.A., "Least-Squares Continuous Sensitivity Analysis of an Example Fluid-Structure Interaction Problem," Vol. AIAA-2008-1896, 2008.

[5] Haftka, R.T., and Gürdal, Z., "Elements of structural optimization," *Solid mechanics and its applications,* Vol. 11, Kluwer Academic Publishers, Dordrecht ; Boston, 1992, pp. 481.

[6] Stanley, L.G.D., and Stewart, D.L., "Design sensitivity analysis : computational issues of sensitivity equation methods," *Frontiers in applied mathematics,* Society for Industrial and Applied Mathematics, Philadelphia, 2002, pp. 139.

[7] Phelan, D.G., and Haber, R., B., "Sensitivity analysis of linear elastic systems using domain parameterization and a mixed mutual energy principle," *Computer Methods in Applied Mechanics and Engineering,* Vol. 77, 1989, pp. 31-59.

[8] Dems, K., and Haftka, R.T., "Two Approaches to Sensitivity Analysis for Shape Variation of Structures," *Mech. Struct. & Mach.,* Vol. 16, No. 4, 1988-1989, pp. 501-501-522.

[9] Arora, J.S., Lee, T.H., and Cardoso, J.B., "Structural Shape Design Sensitivity Analysis: A Unified Viewpoint," *AIAA-91-1214-CP,* 1991, pp. 675-675-683.

[10] Bochev, P.B., and Gunzburger, M.D., "Finite Element Methods of Least-Squares Type," *SIAM Review,* Vol. 40, No. 4, 1998, pp. 789--837.

[11] Jiang, B., "The least-squares finite element method : theory and applications in computational fluid dynamics and electromagnetics," *Scientific computation,* Springer, Berlin ; New York, 1998, pp. 418.

[12] Yang, S., and Liu, J., "Analysis of Least Squares Finite Element Methods for A Parameter-Dependent First-Order System," *Numerical Functional Analysis and Optimization,* Vol. 19, 1998, pp. 191-213.

[13] Bramble, J.H., Lazarov, R.D., and Pasciak, J.E., "
Least-squares methods for linear elasticity based on a discrete minus one inner product." *Comput. Methods Appl. Mech. Engrg.,* Vol. 152, 2001, pp. 520--543.

[14] Proot, M. M. J., "The least-squares spectral element method: theory, implementation and application to incompressible flows," 2003,

[15] Cai, Z., Manteuffel, T., McCormick, S., " *First-order system least squares for the Stokes equations, with application to linear elasticity*," *SIAM Journal of Numerical Analysis,* Vol. 34, No. 5, 1997, pp. 1727--1741.

[16] Pontaza, J.P., "Least-squares variational principles and the finite element method: theory, formulations, and models for solid and fluid mechanics," *Finite Elements in Analysis and Design,* Vol. 41, No. 7-8, 2005, pp. 703.

[17] Pontaza, J.P., "Least-squares finite element formulation for shear-deformable shells," *Computer Methods in Applied Mechanics and Engineering,* Vol. 194, No. 21-24, 2005, pp. 2464.

[18] Kayser-Herold, O., and Matthies, H.G., "Least-Squares FEM Literature Review," Institute of Scientific Computing Technical University Braunschweig, 2005-05, Brunswick, Germany, 2005.

[19] Rasmussen, C.C., Canfield, R.A., and Reddy, J.N., "The Least-Squares Finite Element Method Applied to Fluid-Structure Interaction Problems," AIAA, 2007.

[20] Gel'fand, I.M., Fomin, S.V., and Silverman, R.A., "Calculus of variations," Dover Publications, Mineola, N.Y., 2000, pp. 232.
[21] Reddy, J.N., "An introduction to the finite element method," *McGraw-Hill series in mechanical engineering,* McGraw-Hill Higher Education, New York, NY, 2006, pp. 766.
[22] Naylor, A.W., and Sell, G.R., "Linear operator theory in engineering and science," *Applied mathematical sciences,* Vol. 40, Springer-Verlag, New York, 1982, pp. 624.
[23] Kayser-Herold, O., "Least-Squares Methods for the Solution of Fluid-Structure Interaction Problems," 2006,
[24] Cook, R.D., Malkus, D.S., and Plesha, M.E., "Concepts and applications of finite element analysis," Wiley, New York, 1989, pp. 630.
[25] Šolin, P., Segeth, K., and Doležel, I., "Higher-order finite element methods," *Studies in advanced mathematics,* Chapman & Hall/CRC, Boca Raton, FL, 2004, pp. 382.
[26] Szabo, B.A., and Babuška, I., "Finite element analysis," Wiley, New York, 1991, pp. 368.
[27] Karniadakis, G., and Sherwin, S.J., "Spectralhp element methods for computational fluid dynamics," *Numerical mathematics and scientific computation,* Oxford University Press, New York, 2005, pp. 657.
[28] Bramble, J.H., Lazarov, R.D., and Pasciak, J.E., "Least-squares for Second-Order Elliptic Problems," *Comput. Methods Appl. Mech. Engrg.,* Vol. 152, 1998, pp. 195--210.
[29] Yang, S., and Liu, J., "Least-squares finite element methods for the elasticity problem," *Journal of Computational and Applied Mathematics,* Vol. 87, No. 1, 1997, pp. 39-60.
[30] Cai, Z., and Starke, G., "First-order system least squares for the stress-displacement formulation: Linear elasticity," *SIAM Journal of Numerical Analysis,* Vol. 41, No. 2, 2003, pp. 715--730.
[31] Kim, S.D., Manteuffel, T.A., and McCormick, S.F., "First-order system Least-Squares (FOSLS) for Spatial Linear Elasticity: Pure Traction," *SIAM Journal of Numerical Analysis,* Vol. 38, No. 5, 2000, pp. 1454--1482.
[32] Rasmussen, C.C., "Nonlinear Transient Gust Response Using A Fully-Coupled Least-Squares Finite Element Formulation For Fluidstructure Interaction," Ph.D. dissertation, AFIT, 2008.
[33] Arnold, D.N., "MIXED FINITE ELEMENT METHODS FOR ELLIPTIC PROBLEMS," *Comput. Methods Appl. Mech. Engrg.,* Vol. 82, 1990, pp. 281-281-300.
[34] Speziale, C.G., "Turbulence modeling in non-inertial frames of reference," NASA, ICASE 88-18 (NASA-CR 181646), NASA Langley Research Center, Hampton VA, 1988.
[35] Wickert, D.P., Canfield, R.A., and Reddy, J.N., "Continuous Sensitivity Analysis Methods of Transient Fluid-Structure Interaction Problems using Least-Squares Finite Elements," to be published.
[36] Reddy, J.N., "Applied functional analysis and variational methods in engineering," McGraw-Hill, New York, 1986, pp. 546.

Downloaded by USAF ACADEMY MCDERMOTT LIBR. on November 30, 2021 | http://arc.aiaa.org | DOI: 10.2514/6.2008-1797